

## A Theoretical Study of the Mechanism for the Biogenesis of Cofactor Topaquinone in Copper Amine Oxidases

Rajeev Prabhakar\* and Per E. M. Siegbahn

Contribution from the Department of Physics, Stockholm Centre for Physics, Astronomy and Biotechnology (SCFAB), Stockholm University, S-106 91 Stockholm, Sweden

Received February 17, 2003; E-mail: raju@physto.se

**Abstract:** In the present quantum chemical study, the biogenesis of the cofactor topaquinone (TPQ) has been studied using hybrid density functional theory (B3LYP). The suggested mechanism is divided into six steps and incorporates the observation of four crystallized intermediates. The experimental suggestion that the formation of the Cu(II)-peroxy species is the rate-limiting step is consistent with the results of the present study. Before the formation of the Cu(II)-peroxy species, dioxygen is suggested to first bind at the equatorial position on the copper metal center. A mechanism for the critical O–O bond cleavage is suggested, and this step is found to be driven by an unusually large exothermicity. A complex, spin-forbidden formation of H<sub>2</sub>O<sub>2</sub> with and without the involvement of the copper metal center is discussed. The results are discussed in detail, and comparisons are made to experimental findings and suggestions.

### I. Introduction

Copper-containing amine oxidases (CAOs) constitute a family of redox active enzymes, which is ubiquitous in aerobic organisms, present both in eukaryotes and prokaryotes. In eukaryotes, CAOs have thus far been described in yeast, plants, and mammals. They catalyze the two-electron oxidative deamination of primary amines by dioxygen into corresponding aldehydes, ammonia, and hydrogen peroxide. In prokaryotes, amine oxidases are suggested to have nutrient-associated functions,<sup>1–3</sup> but in eukaryotes they are involved in a large variety of functions. In yeast, this enzyme provides the source of nitrogen and carbon. In plants, they are implicated in lignification, wound healing, and signal transduction.<sup>4</sup> In mammals, they may be involved in tissue differentiation, tumor growth, and programmed cell death.<sup>5,6</sup> One of the reaction products of CAOs, hydrogen peroxide, is suggested to play a role in cell regulation by acting as an intracellular second messenger. It has been shown that hydrogen peroxide can act as a signal-transducing molecule in vascular smooth muscles, evoking responses that include tyrosine phosphorylation, MAP kinase stimulation, and DNA synthesis.<sup>7</sup> The semicarbazide sensitive amine oxidase (SSAO), which is found in the endothelium, has been shown to mediate lymphocyte binding to the

endothelium.<sup>8,9</sup> SSAO activities have been found to be increased in patients with diabetes, atherosclerosis, and heart failures.<sup>10,11</sup>

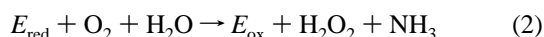
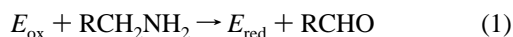
The CAO enzymes are homodimeric with 70–95 kDa subunits, and the crystal structures from *Escherichia coli* (ECAO),<sup>12</sup> pea seedling (PSAO),<sup>13</sup> *Arthobacter globiformis* (AGAO),<sup>14</sup> and yeast *Hansenula polymorpha* (HPAO)<sup>15</sup> have been solved. Recently, Zn- and Co-substituted structures from HPAO have also been crystallized.<sup>16,17</sup> All CAOs contain a peptide-bound quinone cofactor, 2,4,5-trihydroxyphenylalanine-quinone referred to as topaquinone (TPQ), that catalyzes the oxidative deamination of primary amines.<sup>18</sup> This cofactor belongs to a unique class of quinone cofactors that are derived by post-translational modifications of polypeptide-bound amino acid side chains. It has been established that TPQ is synthesized by post-translational modification of a specific tyrosyl residue occurring in the highly conserved Asn-Tyr(TPQ)-(Asp/Glu)-Tyr consensus sequence.<sup>19–21</sup> Two possible mechanisms have

- (1) Parrott, S.; Jones, S.; Cooper, R. A. *J. Gen. Microbiol.* **1987**, *133*, 347–351.
- (2) Cooper, R. A.; Knowles, P. F.; Brown, D. E.; McGuirl, M. A.; Dooley, D. M. *Biochem. J.* **1992**, *288*, 337–340.
- (3) Hacısalihoğlu, A.; Jongejan, J. A.; Duine, J. A. *Microbiology* **1997**, *143*, 505–512.
- (4) McIntire, W. S.; Hartmann, C. *Principles and Application of Quinoproteins*; Davidson, V. L., Ed.; Marcel Dekker: New York, 1993; pp 97–171.
- (5) Morgan, D. L. M. *Methods Mol. Biol.* **1998**, *79*, 3–30.
- (6) Ha, H. C.; Woster, J. D.; Yager, J. D.; Casero, R. A. *Proc. Natl. Acad. Sci. U.S.A.* **1997**, *94*, 11557–11562.
- (7) Sundaresan, M.; Yu, Z.; Ferrans, V. J.; Irani, K.; Finkel, T. *Science* **1995**, *270*, 296–299.

- (8) Bono, P.; Salmi, M.; Smith, D. J.; Jalkanen, S. *J. Immunol.* **1998**, *160*, 5563–5571.
- (9) Salmi, M.; Jalkanen, J. *Exp. Med.* **1996**, *183*, 17–27.
- (10) Murray, J. M.; Saysell, C. G.; Wilmot, C. M.; Tambyrajah, W. S.; Jaeger, J.; Knowles, P. F.; Phillips, S. E. V.; McPherson, M. J. *Biochemistry* **1999**, *38*, 8217–8227.
- (11) Boomsma, F.; van Veldhuisen, D. J.; deKam, P. J.; Manintveld, A. J.; Mosterd, A.; Lie, K. I.; Schalekamp, M. *Cardiovasc. Res.* **1997**, *33*, 387–391.
- (12) Parsons, M. R.; Convery, M. A.; Wilmot, C. M.; Yadav, K. D. S.; Blakeley, V.; Corner, A. S.; Phillips, S. E. V.; McPherson, M. J.; Knowles, P. F. *Structure* **1995**, *3*, 1171–1184.
- (13) Kumar, V.; Dooley, D. M.; Freeman, C. H.; Guss, J. M.; Harvy, I.; McGuirl, M. A.; Wilce, M. C. J.; Zubak, V. M. *Structure* **1996**, *4*, 943–955.
- (14) Wilce, M. C. J.; Dooley, D. M.; Freeman, C. H.; Guss, J. M.; Matsunami, H.; McIntire, W. S.; Ruggiero, C. E.; Tanizawa, K.; Yamaguchi, H. *Biochemistry* **1997**, *36*, 16116–16133.
- (15) Li, R.; Klinman, J. P.; Mathews, F. S. *Structure* **1998**, *6*, 293–307.
- (16) Chen, Z.; Schwartz, B.; Williams, N. K.; Li, R.; Klinman, J. P.; Mathews, F. S. *Biochemistry* **2000**, *39*, 9709–9717.
- (17) Mills, S. A.; Goto, Y.; Su, Q.; Plastino, J.; Klinman, J. P. *Biochemistry* **2002**, *41*, 10577–10584.
- (18) Davidson, V. L. *Principles and Application of Quinoproteins*; Marcel Dekker: New York, 1993; pp 3–14.

been advanced for this process: the enzymatic mechanism, which involves post-translational modification enzyme(s) or a self-catalytic mechanism which involves the amine oxidase-bound copper complex.<sup>20,22</sup> Experiments conducted in the recombinant yeast methylamine oxidase ruled out the enzymatic mechanism.<sup>22</sup> These experiments showed that if the TPQ biogenesis is enzyme-catalyzed then these enzyme(s) would be expected to have higher specificity than CAOs, i.e., the enzymes specific for TPQ formation. It has been observed that the consensus amino acid sequence is present in a large number of proteins which do not contain quinone moieties;<sup>23,24</sup> therefore, consensus amino acid sequence alone is not sufficient to determine the specificity of recognition, whereas the modification of precursor tyrosine through a self-processing mechanism has been observed in several proteins.<sup>25–27</sup> CAOs are thus suggested to be dual-function enzymes, capable of catalyzing both formation of TPQ through the oxygenation of tyrosine and oxidation of amines within a single active site.

The catalytic mechanism is of ping-pong type occurring in two half-reactions known as the reductive and oxidative half-reactions, shown in eqs 1 and 2, respectively:



In the reductive half-reaction, TPQ is reduced by the substrate amine to an aminophenol species, which is reoxidized back to TPQ by molecular oxygen in the oxidative half-reaction. All known CAOs have a highly conserved active site in which a Cu atom is coordinated to the imidazole side chains of three histidines and two water molecules in a distorted square-pyramidal geometry. The crystal structure for the active site of HPAO is shown in Figure 1.

In contrast to the vast amount of information provided by experimental and theoretical studies about catalysis,<sup>28–36</sup> much less has been known about biogenesis. Several studies have addressed the mechanism of TPQ biogenesis by means of nonenzymatic models.<sup>37,38</sup> However, recent spectroscopic, kinetic, and crystallographic studies made it possible to suggest

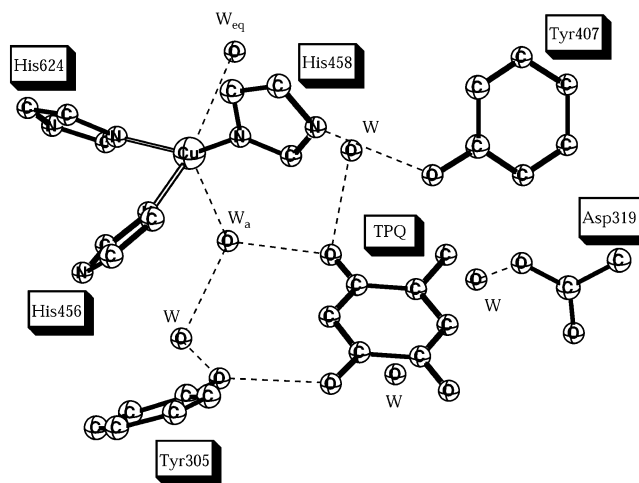


Figure 1. X-ray structure of the active site region of HPAO.

a plausible mechanism for the biogenesis of TPQ.<sup>39–42</sup> An important breakthrough also came from a very recent X-ray crystallographic study of the enzyme from AGAO in which five intermediates in the proposed self-catalytic mechanism of TPQ biogenesis had been crystallized.<sup>43</sup> The mechanism for the biogenesis of cofactor TPQ has been reviewed several times.<sup>44–46</sup> The presence of copper is suggested to be crucial for biogenesis. No other metal has been found to replace copper in TPQ formation. Zinc, cobalt, and nickel have been tried. This is unlike catalysis, where some other metals such as cobalt are also active.<sup>47,48</sup> The consensus residues are also expected to play important roles in TPQ formation. Mutant studies of HPAO showed that the rate of the reaction with O<sub>2</sub> was found to be reduced 6-fold in the E406Q mutant and by more than 30-fold in N404D.<sup>40</sup> In another study, the H624C mutant also significantly reduced the rate of reaction with O<sub>2</sub>. In this case, a ligand-to-metal charge transfer (LMCT) tyr-copper complex was still found to be formed.<sup>39</sup>

The most accepted experimentally suggested mechanism is shown in Figure 2. The mechanism is divided into six steps. In the first step, copper binds anaerobically to the enzyme. To determine the kinetic significance of Cu binding, experiments were conducted with and without prebound Cu(II), and in both cases biogenesis was found to occur with the same rate, showing that Cu(II) binding is a fast process in comparison to biogenesis.<sup>40</sup> Mutant experiments show that the rate of TPQ formation is significantly diminished for the E406Q and N404D mutants,<sup>40</sup> which are known to be important in controlling the conformation

- (19) Mu, D.; Janes, S. M.; Smith, A. J.; Brown, D. E.; Dooley, D. M.; Klinman, J. P. *J. Biol. Chem.* **1992**, *267*, 7979–7982.  
 (20) Mu, D.; Medzihradsky, K. F.; Adams, G. W.; Mayer, P.; Hines, W. M.; Burlingame, A. L.; Smith, A. J.; Cai, D.; Klinman, J. P. *J. Biol. Chem.* **1994**, *269*, 9926–9932.  
 (21) Yoon-Ho, C.; Matsuzaki, R.; Suzuki, S.; Tanizawa, K. *J. Biol. Chem.* **1996**, *271*, 22598–22603.  
 (22) Cai, D.; Klinman, J. P. *Biochemistry* **1994**, *33*, 7647–7653.  
 (23) Bruinberg, P. G.; Evers, M.; Waterham, H. R.; Kuipers, J.; Arnberg, A. C.; Ab, G.; *Biochim. Biophys. Acta* **1989**, *1008*, 157–167.  
 (24) Mu, D. Ph.D. Thesis, University of California, Berkeley, CA, 1993.  
 (25) Waite, J. H. *J. Biol. Chem.* **1983**, *258*, 2911–2915.  
 (26) Waite, J. H.; Rice-Ficht, A. C. *Biochemistry* **1987**, *26*, 7819–7825.  
 (27) Waite, J. H.; Rice-Ficht, A. C. *Biochemistry* **1989**, *28*, 6104–6110.  
 (28) Hartmann, C.; Brzovic, P.; Klinman, J. P. *Biochemistry* **1993**, *32*, 2234–2241.  
 (29) Cai, D.; Dove, J.; Nakamura, N.; Sanders-Loehr, J.; Klinman, J. P. *Biochemistry* **1997**, *36*, 11472–11478.  
 (30) Su, Q.; Klinman, J. P. *Biochemistry* **1998**, *37*, 12513–12525.  
 (31) Hevel, J. M.; Mills, S. A.; Klinman, J. P. *Biochemistry* **1999**, *38*, 3683–3693.  
 (32) Dooley, D. M.; McGuire, M. A.; Brown, D. E.; Turowski, P. N.; McIntire, W. S.; Knowles, P. F. *Nature* **1991**, *349*, 262–264.  
 (33) Prabhakar, R.; Siegbahn, P. E. M. *J. Phys. Chem. B* **2001**, *105*, 4400–4408.  
 (34) Prabhakar, R.; Siegbahn, P. E. M. *J. Comput. Chem.* **2003**, *24*, 1599–1609.  
 (35) Prabhakar, R.; Siegbahn, P. E. M. *J. Phys. Chem. B* **2003**, *107*, 3944–3953.  
 (36) Prabhakar, R.; Siegbahn, P. E. M.; Minaev, B. F.; Ågren, H. To be submitted for publication.

- (37) Mandal, S.; Lee, Y.; Purdy, M. M.; Sayre, L. M. *J. Am. Chem. Soc.* **2000**, *122*, 3574–3584.  
 (38) Rinaldi, A. C.; Ponticelli, G.; Oliva, S.; Di Giulio, A.; Sanjust, E. *Bioorg. Med. Chem. Lett.* **2000**, *10*, 989–992.  
 (39) Dove, J. E.; Schwartz, B.; Williams, N. K.; Klinman, J. P. *Biochemistry* **2000**, *39*, 3690–3698.  
 (40) Schwartz, B.; Dove, J. E.; Klinman, J. P. *Biochemistry* **2000**, *39*, 3699–3707.  
 (41) Schwartz, B.; Olgin, A. K.; Klinman, J. P. *Biochemistry* **2001**, *40*, 2954–2963.  
 (42) Rinaldi, A. C.; Rescigno, A.; Rinaldi, A.; Sanjust, E. *Bioorg. Chem.* **1999**, *10*, 253–288.  
 (43) Kim, M.; Okajima, T.; Kishishita, S.; Yoshimura, M.; Kawamori, A.; Tanizawa, K.; Yamaguchi, H. *Nat. Struct. Biol.* **2002**, *9*, 591–596.  
 (44) Klinman, J. P. *J. Biol. Chem.* **1996**, *271*, 27189–27192.  
 (45) Klinman, J. P. *Chem. Rev.* **1996**, *96*, 2541–2561.  
 (46) Dooley, D. M. *J. Biol. Inorg. Chem.* **1999**, *4*, 1–11.  
 (47) Matsuzaki, R.; Fukui, T.; Sato, H.; Ozaki, Y.; Tanizawa, K. *FEBS Lett.* **1994**, *351*, 360–364.  
 (48) Cai, D. Y.; Williams, N. K.; Klinman, J. P. *J. Biol. Chem.* **1997**, *272*, 19277–19281.

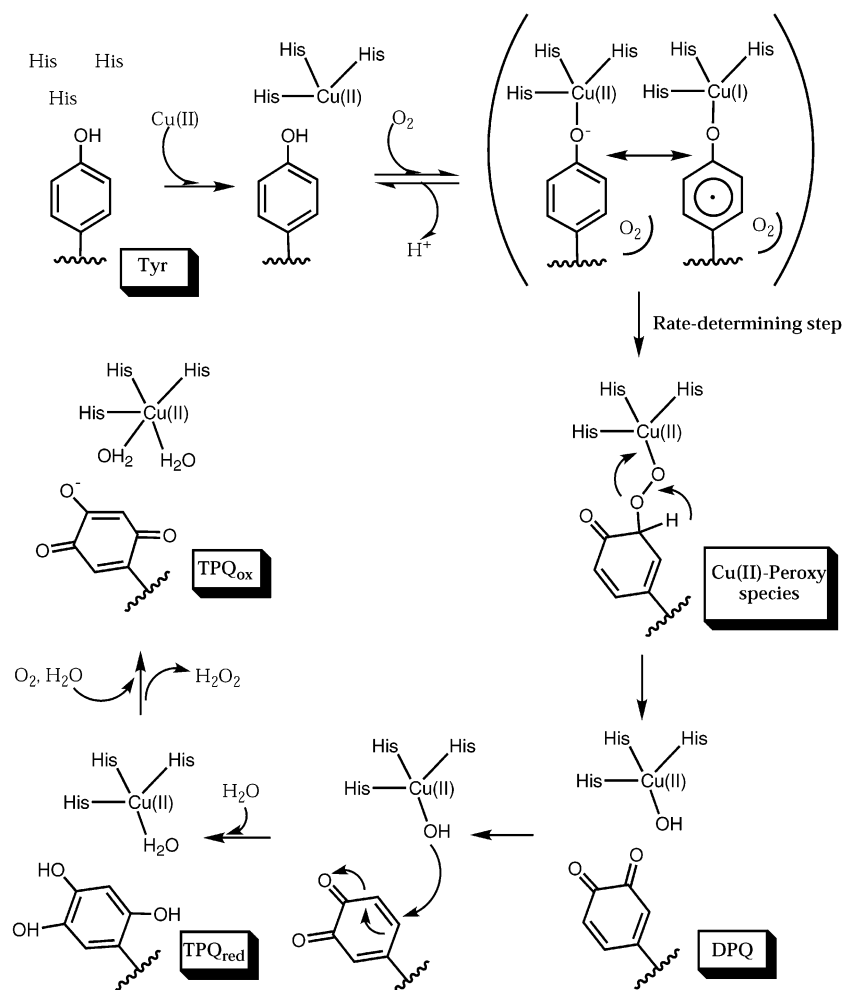


**Figure 2.** Experimentally suggested mechanism for the biogenesis of TPQ in CAO.

of TPQ during catalytic turnover.<sup>49</sup> Intermediate A (Figure 3) has been crystallized for AGAO at 100 K, and the overall structure was found to closely resemble the holo enzyme at the same temperature<sup>43</sup> and also the apo and holo-AGAO at room temperature.<sup>14</sup> At the copper metal center, the precursor tyrosine has access to two possible binding sites on copper: an axial site and an equatorial site. Crystal structures of a Zn-containing analogue of apo-Cu HPAO with an inhibitor azide showed that the precursor tyrosine binds to the metal at the axial position.<sup>16,41</sup> It was suggested earlier by a kinetic analysis of TPQ biogenesis in HPAO that the precursor tyrosine initially does not interact with copper to form a charge transfer complex. Only after the inclusion of dioxygen does it get deprotonated and binds to copper.<sup>40</sup> In the crystal structure of A from AGAO (Figure 3), the hydroxyl group of the side chain of Tyr382 is anaerobically bonded to copper at an axial position with a Cu–O distance of ca. 2.6 Å. The distance of 2.6 Å is longer than that required of <2.0 Å to permit charge transfer, but is still enough for forming a weak bond through charge dipole interaction.<sup>40</sup> The main reason behind the absence of charge transfer could be that Tyr382 is protonated. Other important features of this structure are the flexibility of His592, which could be modeled in two conformations, and the coordination of the copper atom with three histidine residues in a trigonal pyramidal geometry,

consistent with the EPR signal detected for Cu(II) after anaerobic mixing in the enzyme. Structure A can be described as a Cu(II)-tyrosinate species with partial Cu(I)-tyrosyl radical character, as a result of the covalency of the ligand–metal bond which promotes the reaction with dioxygen.<sup>50</sup>

In the second step of the suggested mechanism, dioxygen binds at a site near the precursor tyrosine. The absence of solvent viscosity effects suggests that oxygen prebinds with a weak affinity to the protein rather than reacting in a diffusion controlled manner.<sup>40</sup> Two possible dioxygen binding locations have been suggested: either a vacant equatorial position at the copper metal center<sup>14</sup> or a nonmetal site.<sup>39,40</sup> It has been shown experimentally that during TPQ formation 2 equiv of dioxygen are consumed,<sup>51</sup> and the first O<sub>2</sub> is observed to react more slowly than the second one.<sup>40</sup> It has clearly been indicated by kinetic data that a step, which takes place either simultaneously or precedes the reaction of the first equivalent of O<sub>2</sub>, is rate-limiting in TPQ biogenesis.<sup>40</sup> The above results suggest that neither copper binding nor concomitant O<sub>2</sub> binding and LMCT complex formation are rate-limiting. These results leave either the reaction between the LMCT species and O<sub>2</sub> or an undetermined conformational change as a possible rate-limiting step in the biogenesis. The latter was ruled out by a comparison between the crystal structures of the apo and holo-enzymes, which

(49) Schwartz, B.; Green, E. L.; Sanders-Loehr, J.; Klinman, J. P. *Biochemistry* **1998**, *37*, 16591–16600.

(50) Cox, D. D.; Que, L., Jr. *J. Am. Chem. Soc.* **1988**, *110*, 8085–8092.

(51) Ruggiero, C. E.; Dooley, D. M. *Biochemistry* **1999**, *38*, 2892–2898.

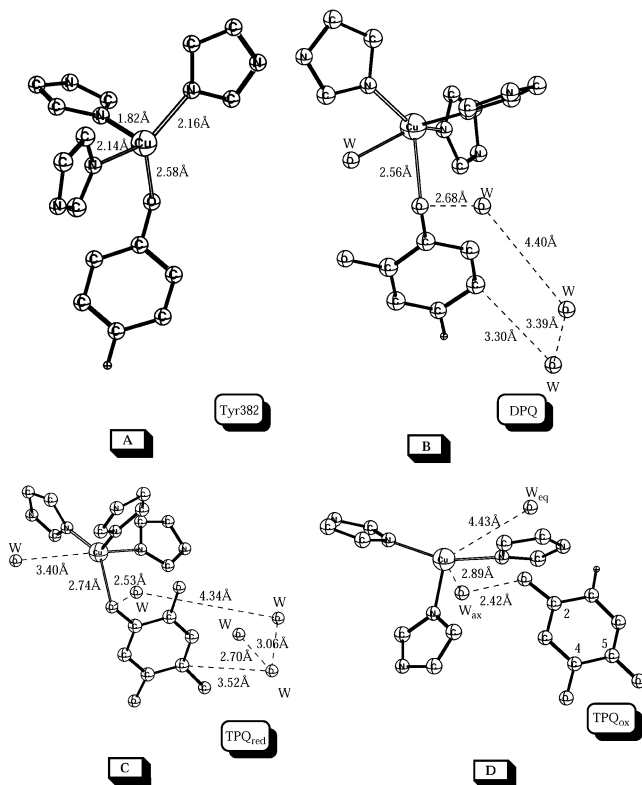


**Figure 3.** X-ray structures of the four intermediates in AGAO.

showed no significant conformational change.<sup>14</sup> In subsequent observations it was found that in HPAO, the assignment of the pH effects to the Y405 is most consistent with a rate enhancement if the LMCT complex includes a deprotonated precursor tyrosine.<sup>40</sup> Furthermore, in the H624C mutant studies of HPAO, the reduction of the rate of TPQ formation could be attributed to the changes in the electronic configuration of the LMCT species, rather than conformational changes at the active site.<sup>39</sup> The experimentally measured rate for TPQ formation of  $12.3 \text{ M}^{-1} \text{ s}^{-1}$  at low pH corresponds to a rate-limiting barrier of 16.0 kcal/mol, and the rate of  $77.8 \text{ M}^{-1} \text{ s}^{-1}$  at high pH corresponds to a barrier of 14.9 kcal/mol. This pH dependence and other factors suggest a direct reaction between the LMCT complex and dioxygen to be rate-limiting in TPQ formation.<sup>40</sup>

In the suggested third step, dioxygen is proposed to react with the Cu(II)-tyrosinate species and form a bridging peroxy intermediate. This intermediate is expected to be stabilized either by an accompanying proton transfer or by electrostatic interactions. The absence of significant solvent isotope effects shows that a proton transfer is not rate-limiting and must be uncoupled to the reaction between the LMCT species and dioxygen.<sup>40</sup> All these results indicate that the formation of the peroxy bridging intermediate is the rate-limiting step in TPQ biogenesis. This intermediate then breaks down to form the product dopaquinone (DPQ) and Cu(II)-hydroxide species. A structure containing the product DPQ has been crystallized in AGAO<sup>43</sup> (see structure B in Figure 3). In the crystal structure, the C-5 position of the TPQ ring is oxidized and O4 of DPQ is bonded axially to the copper atom with a bond distance of 2.6 Å.

In the suggested fourth step, the DPQ ring first rotates 180° around the C $\beta$ –C $\gamma$  bond so that the C-2 position of TPQ faces the Cu metal center. In this position, it is set up for a nucleophilic

attack by a copper-coordinated water or hydroxide.<sup>52</sup> In the suggested fifth step, the C-2 site of TPQ is oxidized. Since the oxygen required for the C-2 oxidation is known to be derived from a water molecule and not from dioxygen,<sup>52</sup> a water exchange reaction is also suggested to take place. The reduced form of the cofactor, TPQ<sub>red</sub>, is formed in this step. In the crystal structure of the product (see structure C in Figure 3), the C-4 hydroxyl group is still coordinated to the copper with a bond distance of 2.74 Å.<sup>43</sup> In the final step of the mechanism, dioxygen enters, and hydrogen peroxide is formed. During this step, the TPQ ring rotates around both the C $\alpha$ –C $\beta$  and C $\beta$ –C $\gamma$  bonds. This rearrangement in the Cu metal center may be important for the binding and release of hydrogen peroxide from the axial position.<sup>53</sup>

In the structures of all the intermediates crystallized in AGAO, the consensus residues Asn381 and Asp383 stay at the same positions, indicating that the orientation of the TPQ ring is not due to the movement of these residues but rather due to the rotation around the C $\alpha$ –C $\beta$  and C $\beta$ –C $\gamma$  bonds. Very recently, the presence of a divalent metal ion has been suggested to play an important role in the TPQ<sub>red</sub> oxidation.<sup>54</sup> A large amount of experimental information combined with the crystal structures of different intermediates have laid down a perfect foundation for the present quantum chemical study of the mechanism. Apart from testing the suggested mechanisms, quantum chemical calculations can contribute by providing additional information about short-lived intermediates and transition states.

## II. Computational Details

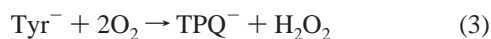
The calculations discussed here were performed using the GAUSSIAN-98<sup>55</sup> and Jaguar<sup>56</sup> programs. The transition states for all the steps and the Hessians for all the structures were calculated using the GAUSSIAN-98 program. The rest of the calculations including the optimization of all the reactants and products were performed using Jaguar. The calculations for the mechanism were performed in two steps. First, an optimization of the geometry was made using the B3LYP method<sup>57</sup> with the double- $\zeta$  quality LACVP basis set. This basis set has an ECP<sup>58</sup> for the copper atom. Open shell systems were treated using unrestricted B3LYP (UB3LYP). In all steps, one atom of each histidine residue was kept frozen from the X-ray structure during the optimization. In the figures, frozen atoms are shown in rectangular boxes. All other degrees of freedom were optimized, and the transition states obtained were confirmed to have only one imaginary frequency of the Hessian. In the second step, the standard LACV3P\*\* basis set

- (52) Nakamura, N.; Matsuzaki, R.; Choi, Y. H.; Tanizawa, K.; Sanders-Loehr, J. *J. Biol. Chem.* **1996**, *271*, 4718–4724.
- (53) Hirota, S.; Iwamoto, T.; Kishishita, S.; Okajima, T.; Yamauchi, O.; Tanizawa, K. *Biochemistry* **2001**, *40*, 15789–15796.
- (54) Kishishita, S.; Okajima, T.; Kim, M.; Yamaguchi, H.; Hirota, S.; Suzuki, S.; Kuroda, S.; Tanizawa, K.; Mure, M. *J. Am. Chem. Soc.* **2003**, *125*, 1041–1055.
- (55) Frisch, M. J.; Trucks, G. W.; Schlegel, H. B.; Scuseria, G. E.; Robb, M. A.; Cheeseman, J. R.; Zakrzewski, V. G.; Montgomery, J. A., Jr.; Stratmann, R. E.; Burant, J. C.; Dapprich, S.; Millam, J. M.; Daniels, A. D.; Kudin, K. N.; Strain, M. C.; Farkas, O.; Tomasi, J.; Barone, V.; Cossi, M.; Cammi, R.; Mennucci, B.; Pomelli, C.; Adamo, C.; Clifford, S.; Ochterski, J.; Petersson, G. A.; Ayala, P. Y.; Cui, Q.; Morokuma, K.; Malick, D. K.; Rabuck, A. D.; Raghavachari, K.; Foresman, J. B.; Cioslowski, J.; Ortiz, J. V.; Stefanov, B. B.; Liu, G.; Liashenko, A.; Piskorz, P.; Komaromi, I.; Gomperts, R.; Martin, R. L.; Fox, D. J.; Keith, T.; Al-Laham, M. A.; Peng, C. Y.; Nanayakkara, A.; Gonzalez, C.; Challacombe, M.; Gill, P. M. W.; Johnson, B. G.; Chen, W.; Wong, M. W.; Andres, J. L.; Head-Gordon, M.; Replogle, E. S.; Pople, J. A. *Gaussian 98*, revision A.7; Gaussian, Inc.: Pittsburgh, PA, 1998.
- (56) JAGUAR 4.1; Schrödinger: Portland, OR, 2000. See: Vacek, G.; Perry, J. K.; Langlois, J.-M. *Chem. Phys. Lett.* **1999**, *310*, 189–194.
- (57) (a) Becke, A. D. *Phys. Rev.* **1988**, *A38*, 3098. (b) Becke, A. D. *J. Chem. Phys.* **1993**, *98*, 1372. (c) Becke, A. D. *J. Chem. Phys.* **1993**, *98*, 5648.
- (58) Hay, P. J.; Wadt, W. R. *J. Chem. Phys.* **1985**, *82*, 299–310.

of triple- $\zeta$  quality was used. This basis set includes one polarization function on each atom and an extended ECP on the copper atom. Zero-point vibrational and thermal effects were added based on B3LYP calculations using the same basis set as for the geometry optimization. Since some atoms were kept frozen, reliable entropy effects could not be obtained, and these effects were therefore excluded in all the steps of the mechanism except the first one. In this step, dioxygen becomes bound, which leads to a significant decrease of entropy by 8.4 kcal/mol which is added to the relative energy. The dielectric effects from the surrounding environment were obtained using the self-consistent reaction field method as implemented in Jaguar.<sup>59,60</sup> A probe radius of  $R = 1.40 \text{ \AA}$  corresponding to the water molecule was chosen. The dielectric constant was set equal to 4, which corresponds to a dielectric constant of about 3 for the protein and 80 for the water medium surrounding the protein.<sup>61</sup> In the present study, models with the same charge were used in all the steps except the last one, which was studied with two different charge states. The relative energies discussed below include all the effects described above. Normal errors of using B3LYP and different aspects of modeling enzyme active sites are described in recent reviews.<sup>62–65</sup>

### III. Results and Discussion

The biogenesis of cofactor TPQ has been studied using similar methods as were used previously in quantum chemical studies of the reductive and oxidative half reactions of CAO.<sup>33–36</sup> The present study is strongly guided by the experimentally suggested mechanism in Figure 2. The first question to be considered here concerns the choice of an appropriate model for the active site. Since in the crystal structures of the intermediates from AGAO<sup>43</sup> the Cu ion is coordinated with three histidines and a tyrosine in a trigonal pyramidal geometry, these ligands are obviously included in the model. In some of the steps, a hydroxyl ion is also bonded to the copper ion in an equatorial position. Histidines are modeled by imidazoles and tyrosine by a *p*-cresol. As experimentally suggested, tyrosine is deprotonated in the first step. The present quantum chemical study of TPQ biogenesis starts from a point where tyrosine is coordinated to copper and the LMCT species has already been formed. Since in comparison to biogenesis the Cu(II) binding is experimentally suggested to be a fast process,<sup>40</sup> it is not investigated in this study. The Cu(II) binding is not expected to have any significant effect on the overall energetics of biogenesis. On the basis of the experimental suggestion that after the Cu(II) binding in the apo enzyme, the precursor tyrosine is in a protonated state,<sup>16,41,43</sup> the overall barrier in the present study is compared to the one measured at high pH. The overall sequence of TPQ formation can be written as:



This reaction is calculated to be exothermic by as much as 99.0 kcal/mol, including zero-point vibrational (plus thermal enthalpy) effects of  $-2.8 \text{ kcal/mol}$ .

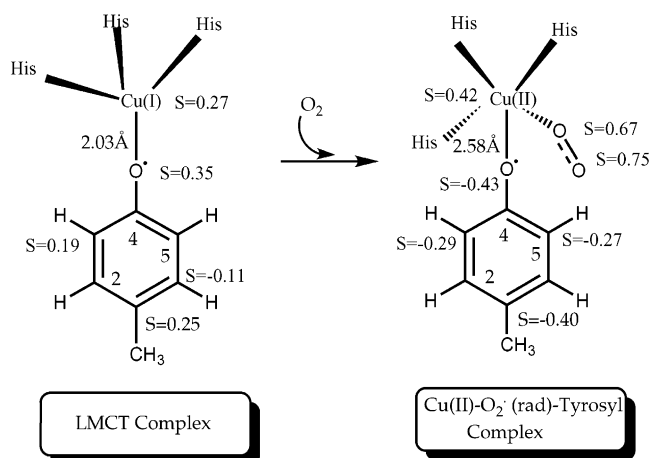


Figure 4. Suggested first step of the mechanism.

**A. Step 1: Dioxygen Binding.** In the first step of the suggested mechanism (Figure 4), dioxygen enters the active site and binds to the LMCT species. After the Cu(II) binding in the apo enzyme, a protonated precursor tyrosine is experimentally suggested to coordinate at the axial position of the copper metal center. It is only during the dioxygen binding that it becomes deprotonated.<sup>16,41,43</sup> The mechanism concerning the simultaneous binding of dioxygen and deprotonation of tyrosine is not clear. Therefore, the present starting point is when the reactant tyrosinate is bound to copper at the axial position forming the LMCT species. In the optimized structure, the Cu–O4 distance is  $2.0 \text{ \AA}$  (Figure 4), which is substantially shorter than the Cu–O4 distance of ca.  $2.6 \text{ \AA}$  for this intermediate in the crystal structure.<sup>43</sup> On optimizing the reactant with a protonated tyrosine the Cu–O4 distance remains unchanged. Furthermore, on taking the coordinates of this intermediate directly from the X-ray structure and optimizing them, the tyrosine residue moves from the axial to the equatorial position, and the Cu–O4 distance still becomes  $2.0 \text{ \AA}$ . It is possible that at the active site the precursor tyrosine is held at an axial position by the active site residues and the backbone. The reactant has significant Cu(I)-tyrosyl character shown by a spin population of 0.3 on copper and 0.7 on tyrosyl, which is in agreement with experimental suggestions.<sup>50</sup> According to experiments, dioxygen can bind at two different locations at the active site, either at an equatorial position on the copper metal center<sup>14</sup> or covalently to the tyrosinate.<sup>39,40</sup> The formation of the Cu(II)-peroxy species has been investigated in both cases and is found to be less favorable by  $11.7 \text{ kcal/mol}$  when dioxygen binds to the tyrosinate. On the basis of this result, dioxygen has been chosen to bind at the equatorial position of the copper metal center. Dioxygen binding at the vacant equatorial position is concomitant with electron transfer from the LMCT species to dioxygen, which leads to the formation of a Cu(II)-superoxide-tyrosyl complex. The formation of this complex is endergonic by  $6.0 \text{ kcal/mol}$ , including solvent effects of  $-2.6 \text{ kcal/mol}$  and a large entropy contribution of  $8.4 \text{ kcal/mol}$ , when free oxygen becomes bound. It has been experimentally observed that Cu(II) cannot be substituted by any other metal, such as  $\text{Zn}^{2+}$ ,  $\text{Co}^{2+}$ ,  $\text{Ni}^{2+}$ ,  $\text{Cd}^{2+}$ , etc., in the TPQ formation; only  $\text{Fe}^{2+}$  was found to have 10% activity.<sup>47,48</sup> At the moment, the reason behind this behavior of the enzyme is not known.

**B. Step 2: Formation of the Cu(II)-Peroxy Species.** In the second step of the suggested mechanism (Figure 5), the tyrosyl-

(59) Tannor, D. J.; Marten, B.; Murphy, R.; Friesner, R. A.; Sitkoff, D.; Nicholls, A.; Ringnalda, M.; Goddard, W. A., III; Honig, B. *J. Am. Chem. Soc.* **1994**, *116*, 11875–11882.

(60) Marten, B.; Kim, K.; Cortis, C.; Friesner, R. A.; Murphy, R. B.; Ringnalda, M.; Sitkoff, D.; Honig, B. *J. Phys. Chem.* **1996**, *100*, 11775–11788.

(61) Blomberg, M. R. A.; Siegbahn, P. E. M.; Babcock, G. T. *J. Am. Chem. Soc.* **1998**, *120*, 8812–8824.

(62) Siegbahn, P. E. M.; Blomberg, M. R. A. *Annu. Rev. Phys. Chem.* **1999**, *50*, 221–249.

(63) Siegbahn, P. E. M.; Blomberg, M. R. A. *Chem. Rev.* **2000**, *100*, 421–437.

(64) Blomberg, M. R. A.; Siegbahn, P. E. M. *J. Phys. Chem.* **2001**, *105*, 9375–9386.

(65) Siegbahn, P. E. M. *Q. Rev. Biophys.* **2003**, *36*, 91–145.

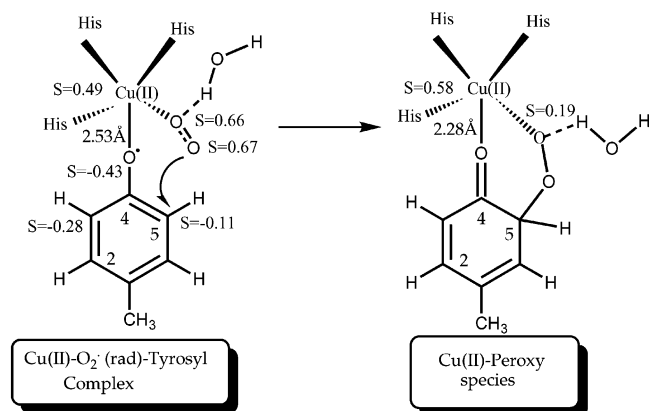


Figure 5. Suggested second step of the mechanism.

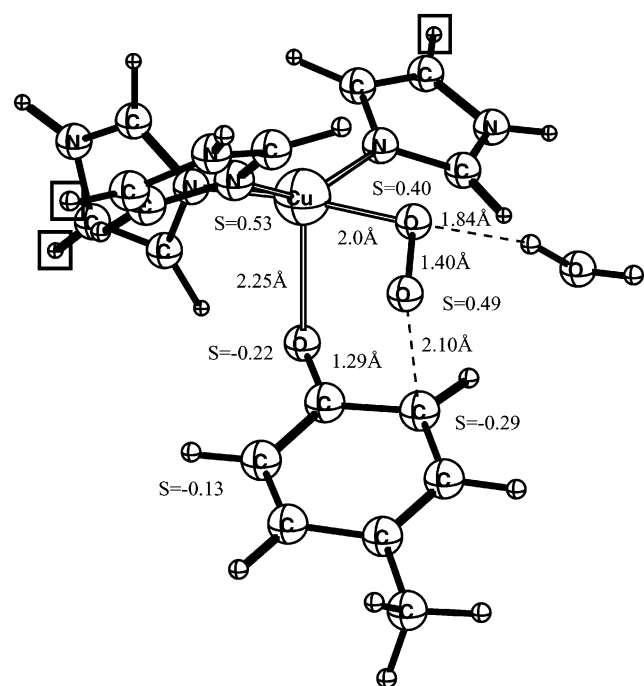


Figure 6. Optimized transition state for step 2.

Cu(II)-superoxide complex formed in the previous step attacks the C-5 position of the TPQ ring, and the bridging Cu(II)-peroxy species is formed. The formation of this species has been suggested experimentally by kinetic studies conducted on CAO from yeast.<sup>40</sup> On the basis of a large number of experiments, it has been concluded that the formation of the peroxo-bridged intermediate is rate-limiting in the TPQ formation (see Introduction). An external water molecule has been added in the model, which stabilizes the superoxide species through a weak hydrogen bond. In this step, an electron transfer from tyrosyl to superoxide is accompanied by a simultaneous attack of superoxide at the C-5 site of TPQ. The optimized transition state for this step is shown in Figure 6, and the calculated barrier is 8.4 kcal/mol, including extremely small solvent effects of  $-0.1$  kcal/mol. It is clearly indicated in the transition-state structure that half of the electron is already transferred. Since this step follows a step which is endergonic by 6.0 kcal/mol, the overall barrier becomes 14.4 kcal/mol, which is in excellent agreement with the experimentally measured one of 14.9 kcal/mol for the rate-limiting step at high pH.<sup>40</sup> This step is exothermic by 11.9 kcal/mol, including solvent effects of  $+0.4$  kcal/mol and zero-point

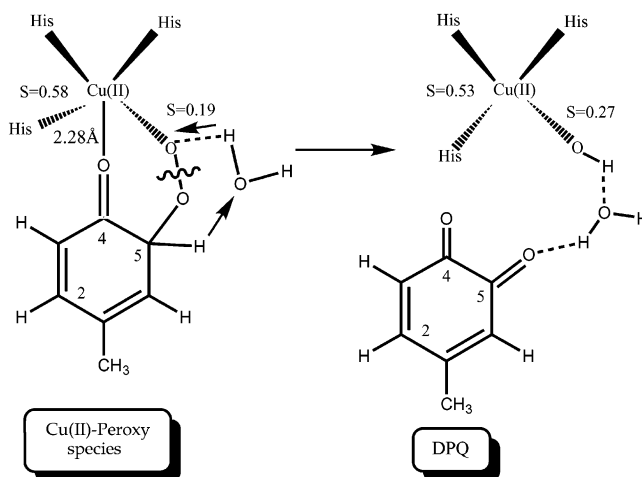


Figure 7. Suggested third step of the mechanism.

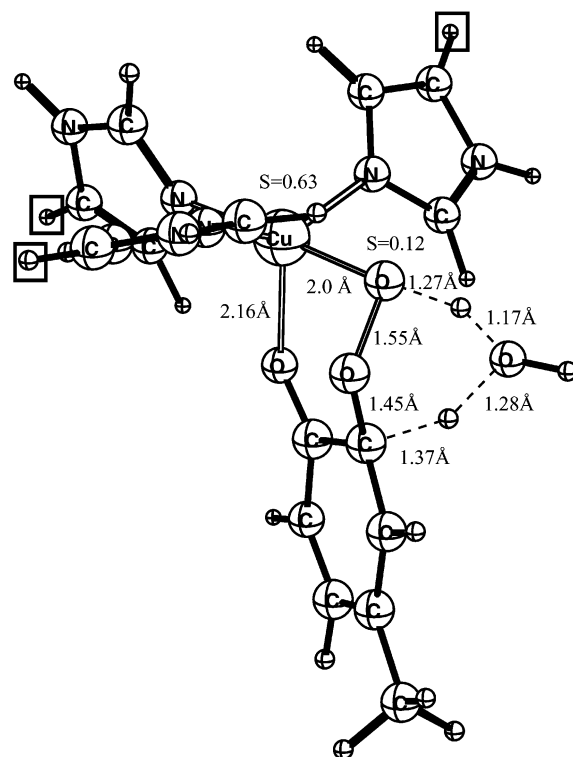


Figure 8. Optimized transition state for step 3.

vibrational (plus thermal enthalpy) effects of  $+1.7$  kcal/mol. In the product, the oxygen atom bound to Cu(II) has a small spin of 0.19, which is stabilized by a water molecule, and the Cu-O4 bond distance is 2.28 Å.

**C. Step 3: Formation of DPQ.** In the third step of the suggested mechanism (Figure 7), the O-O bond of dioxygen is cleaved, thereby establishing the C-5 carbonyl bond. The oxygen atom required for the formation of DPQ is experimentally known to be provided by dioxygen.<sup>52</sup> After the formation of the Cu(II)-peroxy species in the previous step, the O-O bond cleavage can now begin. The optimized transition-state structure is shown in Figure 8, and the computed barrier is 11.4 kcal/mol, including solvent effects of  $-0.7$  kcal/mol and zero-point vibrational (plus thermal enthalpy) effects of  $-4.6$  kcal/mol. As usual, in a heterolytic O-O bond cleavage this is accompanied by proton transfers; in this case indirectly through a water molecule from the  $sp^3$  carbon of the phenol ring to one

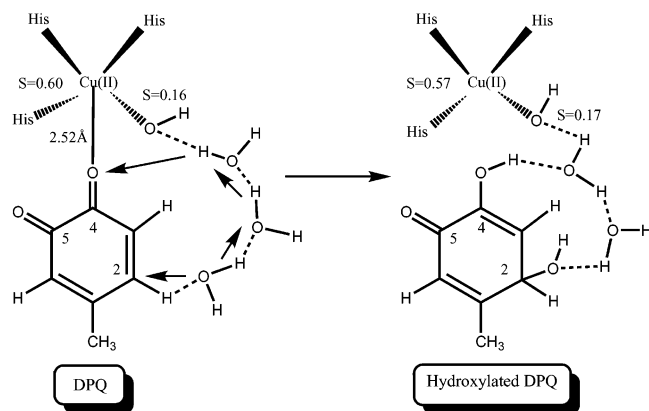


Figure 9. Suggested fourth step of the mechanism.

of the oxygens of the peroxide. In the transition-state structure all the O–H distances are between 1.17 and 1.37 Å, indicating that the proton transfer is concerted. An external water (added to the model in the previous step) assists in this proton transfer. The O–O bond cleavage is driven by an unusually large exothermicity of 55.4 kcal/mol, including a large solvent effect of 8.5 kcal/mol. Shortly after the TS, when the proton has reached the peroxide oxygen, the O–O bond distance starts to increase and the reaction goes to the product without any additional barrier. The absence of solvent isotopic effects rules out the possibility that this proton transfer is rate-limiting.<sup>40</sup> The bound product DPQ has been crystallized in AGAO<sup>43</sup> (Figure 3B). In the X-ray structure, the C-5 position of the TPQ ring is oxidized.

**D. Step 4: Addition of the Hydroxyl Group at the C-5 Position of DPQ.** In the fourth step of the suggested mechanism (Figure 9), a water molecule is activated to attack the C-2 position of TPQ. Before water activation, the DPQ ring is experimentally suggested to rotate by 180° around the C $\beta$ –C $\gamma$  bond.<sup>40</sup> As a result of this rotation, the C-2 position of TPQ is now positioned for an attack by a water or hydroxide coordinated to copper.<sup>52</sup> It has been shown experimentally that the C-2 oxygen of TPQ is derived from a water molecule rather than from dioxygen.<sup>52</sup> In the model, a hydrogen-bonded chain of conserved water molecules is used to connect the Cu-coordinated hydroxide with the C-2 position of TPQ. Since the water molecules are already present at the active site, reaching the structure of the reactant does not require major rearrangements. The reactant of this step has been crystallized (Figure 3B) and resembles the optimized structure. For example, in the crystal structure the Cu–O4 distance is 2.6 Å in comparison to the Cu–O4 distance of 2.52 Å in the optimized structure. In the transition state (Figure 10), a hydroxide group is added to the C-2 position of the TPQ ring while the proton is transferred in a concerted manner to the O-4 position through a hydrogen-bonded chain of water molecules. This step has a barrier of 16.0 kcal/mol, including solvent effects of +3.3 kcal/mol and zero-point vibrational (plus thermal enthalpy) effects of –1.3 kcal/mol. The barrier of 16.0 kcal/mol for this step is slightly higher (1.6 kcal/mol) than the rate-limiting step, which creates a minor disagreement with experiments, since it has been shown that formation of the Cu(II)-peroxy species is rate-limiting. This minor disagreement is in line with the general experience that B3LYP overestimates the activation energy for long-range

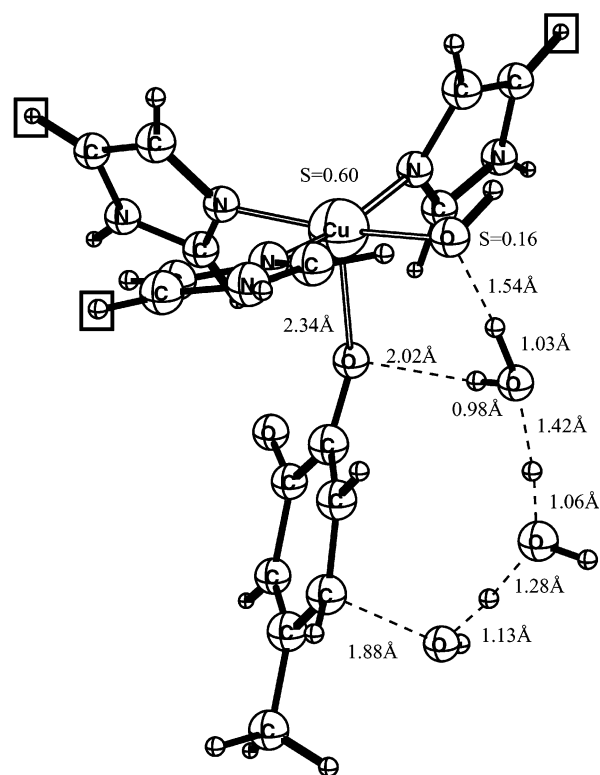


Figure 10. Optimized transition state for step 4.

proton-transfer reactions.<sup>66</sup> The effect of extending the basis set of 9.7 kcal/mol is unusually large. This step is endothermic by 5.4 kcal/mol, and in the product O-4 is not bonded to copper. The endothermicity of this step agrees well with experiments, where the lower energy reactant has been crystallized but not the endothermic product. In the product, the proton from the activated water molecule is not fully transferred to the O-4 site of TPQ, but rather, is positioned between water and O-4. This structure is a real minimum, since the Hessian has no imaginary frequencies. Proton transfer through several ordered water molecules in the enzyme is quite common and has been suggested for proton transfer in, for example, cytochrome-c-oxidase<sup>67</sup> and Ni–Fe hydrogenase.<sup>68</sup> Since the three water molecules are already present at the active site in the X-ray structure (Figure 3B), the loss of entropy should be minor. This step has also been investigated by using only one molecule of intervening water. To do this, a rearrangement is necessary such that Cu(II) is now no longer bonded to the O-4 site of TPQ. The barrier for water activation using one water molecule is found to be only 2.0 kcal/mol higher than with three waters and endothermic by 17.8 kcal/mol. In the product, the enolate species formed is coordinated to Cu(II). After the formation of the enolate species using one water molecule, the protonation of the O-4 site of TPQ could be achieved through some other energetically comparable pathways. However, these pathways have not been investigated in the present study.

**E. Step 5: Formation of TPQ<sub>red</sub>.** In the fifth step of the suggested mechanism, a proton from the C-2 hydroxyl of TPQ

(66) Prabhakar, R.; Blomberg, M. R. A.; Siegbahn, P. E. M. *Theor. Chem. Acc.* **1999**, *104*, 461–470.

(67) Wikström, M.; Verkhovskiy, M. I.; Hummer, G. *Biochim. Biophys. Acta* **2003**, *1604*, 61–65.

(68) Frey, M.; Fontecilla-Camps, J. C.; Volbeda, A. *Handbook of Metalloproteins*; Messerschmidt, A., Huber, R., Poulos, T., Wieghardt, K., Eds.; Wiley: Chichester, U.K., 2001, 880–896.

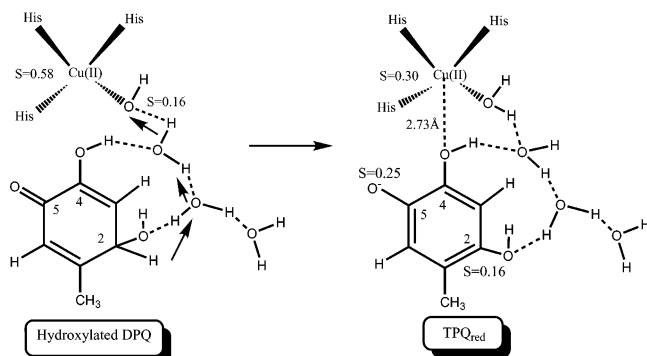


**Figure 11.** Suggested fifth step of the mechanism.

is transferred to the hydroxyl group coordinated to copper. TPQ<sub>red</sub> and a water molecule, coordinated to the Cu(II) ion, are formed (Figure 11). The same hydrogen-bonded chain of water molecules as used in the previous step is used here. In the model, an additional water molecule is added which provides stabilization to the transition state by forming a hydrogen bond with the C-2 hydroxyl group of TPQ. In the crystal structure of this intermediate from AGAO<sup>43</sup> (Figure 3C), a hydrogen bond of this type exists between the C-2 hydroxyl of the cofactor and Thr403. This step has a barrier of 12.6 kcal/mol, including solvent effects of  $-4.8$  kcal/mol and zero-point vibrational (plus thermal enthalpy) effects of  $-2.0$  kcal/mol. Since this step follows a step, which is endothermic by 5.4 kcal/mol, the overall barrier from the resting state of DPQ becomes 18.0 kcal/mol. Here the disagreement with experiments is slightly larger than the one in the previous step, but still not outside the normal error bars of 3–5 kcal/mol. In this step, a long-range proton transfer takes place, which is also slightly overestimated by DFT. In the absence of any deuterium isotope effects, a proton-transfer process cannot be rate-limiting in TPQ formation;<sup>40</sup> thus, the barrier has to be lower than 14.4 kcal/mol. The optimized transition state is shown in Figure 12, where the O–H distances indicate a concerted proton-transfer process. The formation of the product is exothermic by 10.5 kcal/mol, including solvent effects of  $-4.1$  kcal/mol. The exothermicity of the product TPQ<sub>red</sub> is in agreement with experiments, where the low-energy product has been crystallized but not the high-energy reactant. The X-ray and optimized structures are very similar, with a Cu–O4 bond distance of 2.74 Å in the crystal structure in comparison to 2.73 Å in the optimized structure. As with the previous step of water activation using one water molecule, in this step the proton transfer could also be achieved through some other possible reaction pathways. However, the investigation of these alternative pathways is beyond the scope of the present study.

**F. Step 6: Formation of TPQ<sub>ox</sub>.** In the last step of the suggested mechanism, the second oxygen molecule takes two electrons and two protons from TPQ<sub>red</sub> to produce H<sub>2</sub>O<sub>2</sub>. The formation of hydrogen peroxide has been suggested experimentally, and prior to its formation, the TPQ ring is proposed to rotate around both the C $\alpha$ –C $\beta$  and C $\beta$ –C $\gamma$  bonds.<sup>39–41,43</sup> It has been observed very recently that the reduced form of the cofactor (TPQ<sub>red</sub>) is resistant to air oxidation and requires the presence of a divalent metal ion.<sup>54</sup> To investigate the role of Cu(II) in the TPQ<sub>red</sub> oxidation, this step has been investigated both with and without the inclusion of the copper metal center.

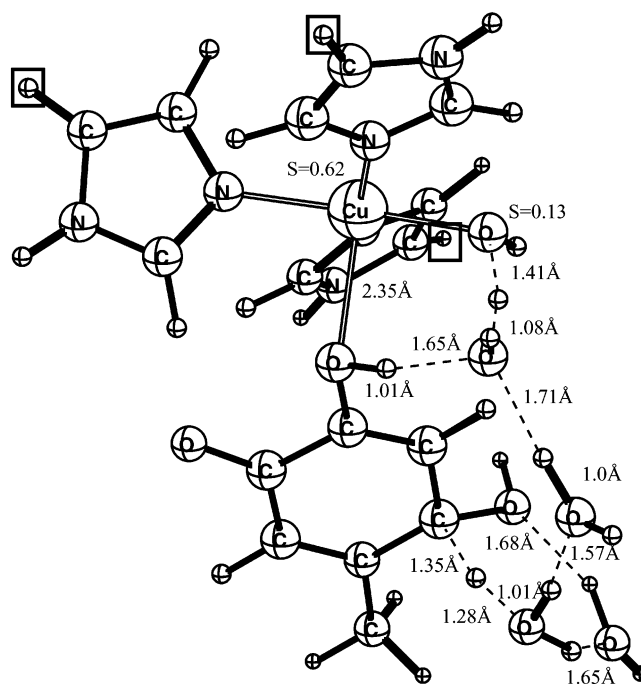
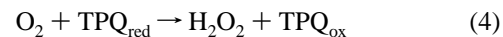


**Figure 12.** Optimized transition state for step 5.

Apart from the copper metal center, TPQ<sub>red</sub>, a chain of two water molecules and dioxygen are also included in the model for this step. The reaction leading to hydrogen peroxide can be written as:



The overall reaction is a spin-forbidden process. TPQ<sub>red</sub>, H<sub>2</sub>O<sub>2</sub>, and TPQ<sub>ox</sub> are all singlets, and O<sub>2</sub> is a triplet. To form hydrogen peroxide, the system has to undergo a triplet (T)  $\rightarrow$  singlet (S) transition. The presence of the divalent metal center could play an important role in overcoming the spin prohibition. The role of a divalent metal in the spin transition induced by exchange interaction in the oxidative half-reaction of CAO has been studied in detail.<sup>36</sup> In this step, dioxygen replaces a water molecule and binds between the O-2 and O-4 positions of the cofactor (Figure 13). According to the B3LYP calculations, the dioxygen binding is accompanied by a simultaneous transfer of two electrons and a proton from the O-2 site of TPQ<sub>red</sub> to the dioxygen. The transfer of two electrons and a proton takes place without any barrier and occurs during the optimization of the reactant. In the reactant, a hydro-peroxy species (O<sub>2</sub>H) is already formed and is bonded to the Cu(II) ion. The concerted transfer of two electrons and a proton is necessary for the low barrier in this step. The absence of any O-18 and deuterium isotope effects confirms that this is a fast process. The formation of this complex could be slightly endergonic due to a binding of free dioxygen. The entropy contribution in this step should be smaller because, unlike the first step, here dioxygen binding is accompanied by a release of a water molecule. After the formation of hydro-peroxy species, the O-4 proton is transferred using the hydrogen-bonding chain of water molecules. This concerted proton transfer leads to the formation of hydrogen peroxide. In the transition state, all the O–H distances are between 1.10 and 1.40 Å, indicating that this process is concerted. This step has a very low barrier of 2.1 kcal/mol, including a solvent effect of  $-3.3$  kcal/mol and zero-point



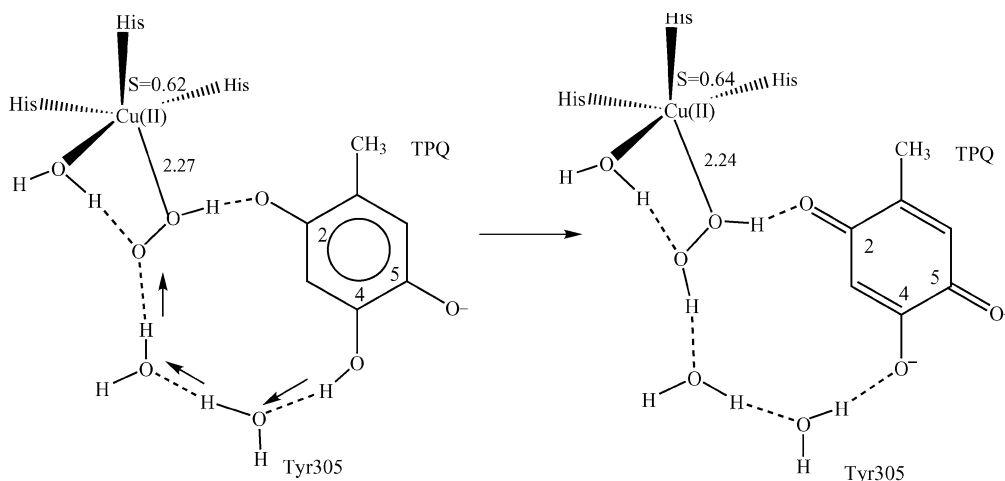


Figure 13. Suggested sixth step of the mechanism.

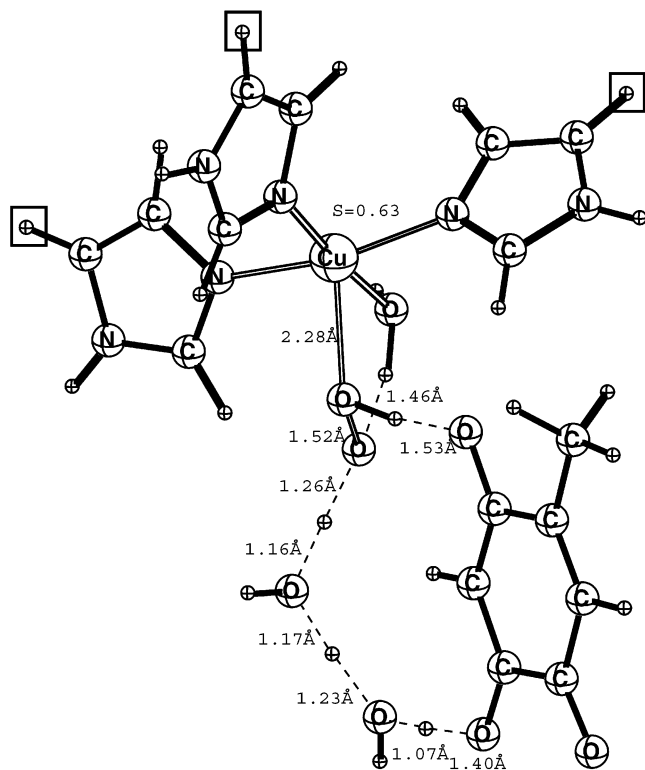


Figure 14. Optimized transition state for step 6.

vibrational (plus thermal enthalpy) effects of  $-3.1$  kcal/mol. The optimized transition state for this step is shown in Figure 14. This step is slightly exothermic by  $3.2$  kcal/mol, and in the product  $\text{H}_2\text{O}_2$  and the oxidized form of cofactor  $\text{TPQ}_{\text{ox}}$  are formed. In the presence of the copper metal center, an alternative mechanism for the formation of  $\text{H}_2\text{O}_2$  has also been investigated. According to this mechanism, dioxygen replaces a water molecule concomitantly with an electron transfer from  $\text{TPQ}_{\text{red}}$  to dioxygen. In the reactant, a  $\text{Cu(I)}$ -superoxide species and a semiquinol form of the cofactor is formed. The formation of this complex is  $27.3$  kcal/mol higher than the reactant (hydroperoxy species) in the suggested mechanism. After the formation of the  $\text{Cu(I)}$ -superoxide species, an electron from the cofactor and O-2 and O-4 protons are transferred in a concerted manner to form  $\text{H}_2\text{O}_2$ . Because the calculated barrier for the alternative mechanism is prohibitively high, this mechanism is ruled out.

It has also been suggested experimentally that the TPQ ring rotates and forms the catalytically active “off-Cu” conformation.<sup>43</sup> On the basis of the experimental suggestion, this step has also been studied without including the copper metal center in the model.  $\text{TPQ}_{\text{red}}$  can have two possible protonation states. In one of them, C-5 of  $\text{TPQ}_{\text{red}}$  has an oxido group, while in the other C-5 has a hydroxyl group. Because neither the protonation state of oxygen at C-5 of  $\text{TPQ}_{\text{red}}$  nor its possible implications on the  $\text{TPQ}_{\text{ox}}$  formation are exactly clear, both these possibilities were explored in the present study. In the first case, C-5 of  $\text{TPQ}_{\text{red}}$  is chosen to have an oxido group, and the whole system is negatively charged. This step is divided into two parts. In the absence of the copper metal center, the mechanism for the  $\text{H}_2\text{O}_2$  formation is essentially the same as suggested previously for hydrogen peroxide formation in glucose oxidase (GO).<sup>69</sup> In the first part, free dioxygen replaces one of the water molecule and binds in a cavity between the O-2 and O-4 positions of  $\text{TPQ}_{\text{red}}$ . The presence of dioxygen at the active site leads to the first electron transfer which is facilitated by weak intermolecular (and O–O) vibrations. This electron transfer leads to the creation of the  $\text{TPQ}(\text{rad})$ –superoxide(rad) radical pair (RP). At this juncture, the radical pair formed is in a triplet state. The superoxide radical has a very large SOC matrix element, which leads to a fast  $T \rightarrow S$  spin transition. This type of transition has been discussed in great detail for GO.<sup>69</sup> The starting point is that the triplet and singlet states are perfectly degenerate.

After the  $T \rightarrow S$  transition, in the second part of this step, the radical pair is in a singlet state. At this stage, the  $\text{TPQ}_{\text{red}}$  radical transfers its O-4 proton to the  $\text{O}_2^-$  radical, which is followed by an electron-coupled proton transfer to the  $\text{O}_2\text{H}$  radical forming  $\text{H}_2\text{O}_2$ . The calculated free energy barrier for this concerted  $2\text{H}^+ + e^-$  transfer process is  $5.1$  kcal/mol. It has to be stressed that such a simultaneous  $2\text{H}^+ + e^-$  transfer can only occur in the singlet state of the whole system. This step leads to the formation of the oxidized form of the cofactor  $\text{TPQ}_{\text{ox}}$  and is exothermic by  $23.0$  kcal/mol.

In the second protonation case, C-5 of  $\text{TPQ}_{\text{red}}$  has a hydroxyl group and the whole system is in a neutral charge state. In this case, the  $\text{TPQ}_{\text{ox}}$  formation follows a slightly different mechanism, in which dioxygen binding is accompanied by an electron-coupled proton transfer from O-2 of  $\text{TPQ}_{\text{red}}$  to dioxygen forming

(69) Prabhakar, R.; Siegbahn, P. E. M.; Minaev, B. F.; Ågren, H. *J. Phys. Chem. B* **2002**, *106*, 3742–3750.

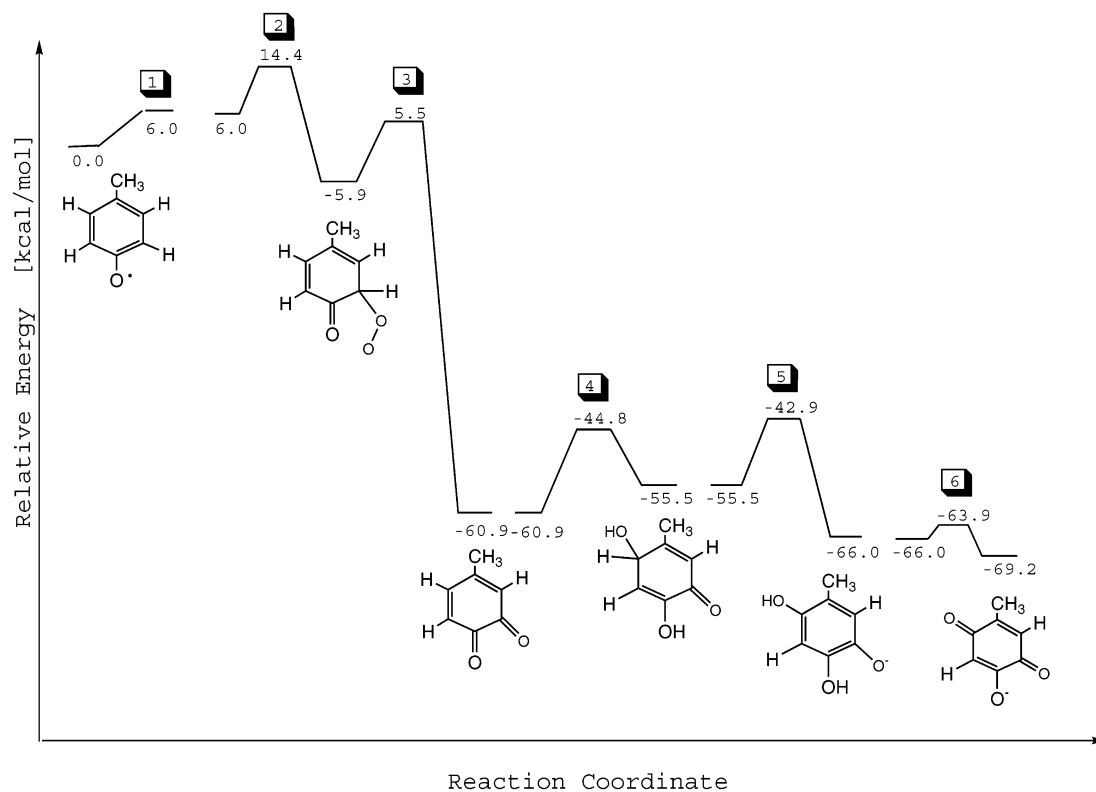


**Figure 15.** Energy diagram for the biogenesis of cofactor TPQ in CAO.

the  $O_2H(\text{rad})\text{--}TPQ(\text{rad})$  radical pair. The RP formed is in a triplet state, and in the same manner as mentioned above the  $T \rightarrow S$  spin transition takes place. In the singlet state of the RP, an electron-coupled proton transfer takes place, but it has a higher barrier by 7.4 kcal/mol and the product is highly endothermic. These results strongly suggest that C-5 of  $TPQ_{\text{red}}$  is favored to have an oxido group. As shown in the crystal structure of the holo enzyme in AGAO (Figure 3D), after the formation of  $TPQ_{\text{ox}}$  the active site rearranges, and Cu becomes pentacoordinated where an additional water molecule occupies the vacant axial position.<sup>43</sup>

#### IV. Summary

The biogenesis of TPQ has been studied using similar kinds of computational methods and models as those used for the reductive half-reaction,<sup>33,34</sup> oxidative half-reaction,<sup>35,36</sup> and different substrate reactions of other enzymes such as RNR<sup>70,71</sup> and PFL.<sup>72</sup> The present quantum chemical study is strongly guided by the vast amount of structural and spectroscopic information provided by experiments. As shown in Figure 15, the energy diagram for the mechanism suggested in the present study can be divided into six steps. This diagram is constructed by imposing the condition that the reactant of each step has the same energy as the product for the previous step. The suggested mechanism starts from a point where an LMCT species has been formed and where the O-4 site of the unprotonated tyrosine is bonded to Cu(II). This species has been crystallized in AGAO.<sup>43</sup> After the formation of this species, the binding of dioxygen takes place. Two possible dioxygen binding locations have been

suggested:<sup>14,39,40</sup> (1) an equatorial position on the copper metal center and (2) an off-Cu location at tyrosinate. It is calculated in the present study that dioxygen is more favorable by 11.7 kcal/mol to bind at the equatorial position on the copper metal center. Dioxygen binds concomitantly with the electron transfer from tyrosinate to dioxygen, and a tyrosyl-Cu(II)-superoxide complex is formed. The formation of this complex is endergonic by 6.0 kcal/mol. In the second step, the C-5 position of the TPQ ring is attacked by the Cu(II)-superoxide complex and a bridging Cu(II)-peroxy species is formed. This step has been studied in great detail by various experimental techniques. It is concluded from the experimental results obtained from kinetic studies,<sup>40</sup> comparing crystal structures of apo and holo-enzymes,<sup>14</sup> conducting H624C mutant experiments,<sup>39</sup> and measuring limiting rates at high and low pH<sup>40</sup> that the formation of the Cu(II)-peroxy species is the rate-limiting step in TPQ formation. The calculated barrier of 14.4 kcal/mol for this step is in perfect agreement with the experimentally measured barrier of 14.9 kcal/mol. This step is exothermic by 11.9 kcal/mol.

In the third step of the suggested mechanism, the critical O–O bond cleavage takes place and a C-5 carbonyl bond is created to form DPQ. Heterolytic O–O bond cleavage is accompanied by a proton transfer and driven by an extremely large exothermicity. This step has a barrier of 11.4 kcal/mol and is 55.4 kcal/mol exothermic. The absence of solvent isotope effects indicates that the accompanying proton transfer in this step is not rate-limiting.<sup>40</sup> The structure of DPQ has been crystallized in AGAO.<sup>43</sup> In the fourth step, a water molecule is activated to add a hydroxyl group at the C-2 position of TPQ. It has been shown experimentally that the C-2 position of TPQ is attacked by a water or hydroxide coordinated to the copper and that the C-5 oxygen of DPQ is derived from a water molecule rather

(70) Siegbahn, P. E. M. *J. Am. Chem. Soc.* **1998**, *120*, 8417–8429.

(71) Himo, F.; Siegbahn, P. E. M. *J. Phys. Chem. B* **2000**, *104*, 7502–7509.

(72) Himo, F.; Eriksson, L. A. *J. Am. Chem. Soc.* **1998**, *120*, 11449–11455.

than dioxygen.<sup>52</sup> This step has a barrier of 16.0 kcal/mol and is endothermic by 5.4 kcal/mol. Due to an overestimation of the barrier for long-range proton-transfer processes in DFT,<sup>66</sup> the barrier for this step is slightly higher than the one in the second step. In the fifth step, a proton transfer from the C-2 hydroxyl group of TPQ to a hydroxyl group coordinated to copper leads to the formation of the reduced form of TPQ<sub>red</sub> and a water molecule. A structure containing the product TPQ<sub>red</sub> has been crystallized in AGAO.<sup>43</sup> This step has a barrier of 12.6 kcal/mol and is exothermic by 10.5 kcal/mol. From the formation of DPQ, the overall barrier for this step becomes 18.0 kcal/mol. The calculated barrier for this step is in minor disagreement with experiments, which is again due to the overestimation of the long-range proton-transfer barrier by DFT.<sup>66</sup> It is clear that in the absence of a measured deuterium isotope effect, this step cannot be rate-limiting.<sup>40</sup> The deviation from experiments is not very large and is within the accuracy of the present methods (3–5 kcal/mol).

In the last step of the suggested mechanism, TPQ<sub>red</sub> donates two electrons and two protons to dioxygen to create the oxidized form of the cofactor, TPQ<sub>ox</sub>. The formation of hydrogen peroxide is a spin-forbidden process in which triplet dioxygen reacts with singlet TPQ<sub>red</sub> to produce singlet H<sub>2</sub>O<sub>2</sub> and TPQ<sub>ox</sub>. To form the products, the hydrogen peroxide and TPQ<sub>ox</sub> system has to undergo a triplet → singlet transition. The presence of the copper metal center is suggested to play a key role in overcoming the spin prohibition. This step has been investigated both with and without the presence of the copper metal center. In the presence of the copper metal center, the dioxygen binding takes place with the simultaneous transfers of two electrons and a proton from the C-2 oxygen of TPQ<sub>red</sub> to dioxygen and a hydro-peroxy species (O<sub>2</sub>H) is formed. After the formation of the hydro-peroxy species, a proton transfer from the O-4 site of TPQ<sub>red</sub> through a hydrogen-bonding chain leads to the formation of H<sub>2</sub>O<sub>2</sub>. This step has a barrier of 2.1 kcal/mol and is exothermic by 3.2 kcal/mol. An alternative mechanism has also been investigated in the presence of the copper metal center.

According to the alternative mechanism, dioxygen binding is accompanied by an electron transfer from TPQ<sub>red</sub> to dioxygen, resulting in the formation of a Cu(I)-superoxide species and a semiquinol form of the cofactor. After the formation of this complex, H<sub>2</sub>O<sub>2</sub> production proceeds through a concerted transfer of an electron and the O-2 and O-4 protons from the TPQ<sub>red</sub>. Since this mechanism is calculated to be energetically unfavorable, it has been ruled out.

In the absence of the copper metal center, the TPQ ring is suggested to be in the catalytically active “off-Cu” conformation.<sup>43</sup> This step has been investigated for two possible protonation states of TPQ<sub>red</sub>, i.e., C-5 of TPQ<sub>red</sub> either has an oxido group or a hydroxyl group. At the starting point, dioxygen occupies a cavity between the O-2 and O-4 positions of TPQ<sub>red</sub>. Dioxygen binding is followed by an electron transfer without any barrier leading to the creation of a triplet TPQ(rad)–superoxide(rad) radical pair. After the formation of the triplet radical pair, spin–orbit coupling and the hindered rotation of the superoxide radical induce the T → S spin transition in the radical pair. Once the radical pair is in the singlet state, TPQ<sub>red</sub>(rad) donates its O-4 proton to the O<sub>2</sub><sup>−</sup> radical followed by a concerted electron-coupled proton transfer to the O<sub>2</sub>H radical to form H<sub>2</sub>O<sub>2</sub>. When C-5 of TPQ<sub>red</sub> has an oxido group, this step has a barrier of 5.1 kcal/mol and is exothermic by 23.0 kcal/mol. In comparison, with a hydroxyl group at C-5 the barrier increases by 7.4 kcal/mol and the product is highly endothermic. In that case, the formation of H<sub>2</sub>O<sub>2</sub> follows a slightly different mechanism.

The model calculations performed in the present study did not only test the already known experimental information but have also given additional information in almost all the steps of the complex mechanism of TPQ biogenesis. This has led to a deeper understanding of this unique enzyme, which is capable of catalyzing the dual processes of TPQ biogenesis and turnover by using a single active site.

JA034721K